Accelerating 4D-Flow Acquisitions by Reducing TE and TR with Optimized RF and Gradient Waveforms

Michael Loecher[1], Patrick Magrath[2], Eric Aliotta[3], and Daniel B Ennis[1,2,3]

[1]*Radiological Sciences, University of California, Los Angeles, CA, United States,* [2]*Bioengineering, University of California, Los Angeles, CA, United States,* [3]*Biomedical Physics, University of California, Los Angeles, CA, United States*

Synopsis

4D-Flow MRI is a powerful technique for simultaneously imaging vascular anatomy and hemodynamics. However, its clinical utility is limited by long (10-20 minute) scan times. This work aims to shorten scan times by using fast RF pulses and convex optimized gradient waveforms. The waveforms are optimized with arbitrary shapes, and are designed to go as fast possible without causing peripheral nerve stimulation by including an additional PNS constraint. The optimized sequence is implemented and tested in flow phantoms and a volunteer. The data acquired with the optimized waveforms is up to 33% faster, with no significant difference in measured data compared to a reference sequence.

Introduction

4D-Flow MRI is a powerful technique for simultaneously imaging vascular anatomy and hemodynamics. However, its clinical utility is limited by long (10-20min) scan times. Advances in parallel imaging and compressed sensing techniques continue, but kernel-level methods to accelerate scanning by optimizing TE and TR are still possible. For decades, the standard method for creating efficient bipolar flow-sensitizing gradients has been based on the analytic work by Bernstein et al.[1]. This work, however, only considers trapezoidal or triangular gradients, and does not account for possible optimizations in the RF waveform, nor peripheral nerve stimulation (PNS). Traditional bipolar design often assumes the use of a single slew rate; however, modern scanners slew so quickly that maximum slew rate flow-encoding bipolars would cause PNS discomfort. Consequently, slew rates are typically derated globally, leading to suboptimal TE and TR. This work aims to evaluate a series of optimization methods (fast RF pulses and PNS-constrained convex optimized gradients) to reduce the TE and TR of 4D-Flow exams, substantially reducing scan times.

Optimizations

RF Optimization – The slab-selective excitation profiles were compared for a standard windowed-sinc RF pulse and a minimum-phase SLR RF pulse [2]. VERSE optimization was also applied to these two pulses to further shorten the RF pulse duration with an equivalent excitation profile[3].

Gradient Optimization – The bipolar gradients were shortened with convex optimization[4]. This method finds the shortest possible gradient waveform of arbitrary shape that satisfies a set of given constraints: 1) hardware limits on gradient amplitude (80mT/m) and slew rate (200T/m/s); 2) target gradient zeroth moments (M_0) for phase encoding, slab-selection rewinding, and readout pre-winding; 3) target gradient first moments (M_1) for velocity encoding; and 4) PNS using the SAFE model for estimating the peripheral nerve response to applied gradients[5]. Additionally, the spoiler gradients were optimized using a similar procedure, but without any constraint on M_1.

Methods

RF Pulse – RF and slab-selection gradients were tested independently of other optimizations on a static phantom to examine excitation profiles, and in a flow phantom with fluid pumped in and out of the slab. Flow values were compared to the standard vendor supplied windowed sinc pulse with Bland-Altman analysis.

RF+Gradient Waveform – The fully optimized sequence (using VERSE min-phase RF) was compared to a vendor supplied reference sequence that used conventional optimizations as in [1]. Optimized TE and TR were compared to the reference sequence over a range of Vencs and resolutions. The optimized sequence was implemented on a 3T scanner (Siemens,Prisma) with the following parameters: Venc=80cm/s, 1.0x1.0x2.0mm^3 resolution, 220x164x64mm FOV, 8°flip, BW=550Hz/px. The optimized sequence was compared to the reference sequence in a flow phantom, in a static phantom for eddy current comparisons, and in vivo in the head of a healthy volunteer. Flow rates were compared with Bland-Altman analysis across multiple planes and ROIs.

Results

RF Pulse – Figure 1 shows the results of the slab-selection comparison where excitation profiles of all the tested methods perform similarly. Flow values are not significantly changed with the use of any of the tested waveforms. The VERSE min-phase SLR pulse is the fastest (0.23ms vs reference 1.0ms).

RF+Gradient Waveform – Figure 2 shows substantial time savings for the optimized RF and gradient waveforms compared to the reference sequence for a given protocol (TR/TE reduction=5.62ms to 3.82ms, 3.11ms to 2.33ms respectively). Figure 3 shows timings from the optimized waveforms compared to the reference over a range of Vencs and resolutions. TE/TR were reduced by 13-38% and 24-33% respectively. Bland Altman analysis of flow-rates in the phantom experiment (Figure 4) shows good agreement. There was no significant difference in VNR between phantom experiments (19.5±0.6 vs 19.3±0.6). Figure 4b shows some increase in the background eddy current phase with the optimized method. Figure 5 shows the results of in vivo validation, where good qualitative or quantitative differences are seen. Due to the shorter TR, an additional segment could be used to reduce scan time by 25% (15:41 to 11:39), while also slightly improving temporal resolution (67ms to 61ms).

Conclusion

This work demonstrates that 4D-Flow scan times can be significantly decreased (TR reduction of up to 33%) with optimization of the RF and gradient waveforms with only a small increase in eddy current error. Currently the largest obstacle to routine implementation is off-line computation, which currently takes 30-120min, which we intend to improve with parallelization and warm-starting. Including a PNS constraint in the optimization allows for a more time efficient usage of the gradient slew-rates. Future work will include a wider range of in vivo validation studies, as well as investigating the effect on higher order motion, mitigating eddy currents, and examining the robustness to off-resonance when using the VERSE pulse.

Acknowledgements

We gratefully acknowledge funding from the UCLA Department of Radiological Sciences and Siemens Healthineers.

References

[1] Bernstein M a, Shimakawa a, Pelc NJ. Minimizing TE in moment-nulled or flow-encoded two- and three-dimensional gradient-echo imaging. J Magn Reson Imaging. 1992;2(5):583–8.

[2] Pauly J, Le Roux P, Nishimura D, Macovski A. Parameter relations for the Shinnar-Le Roux selective excitation pulse design algorithm [NMR imaging]. IEEE Trans Med Imaging. 1991;10(1):53–65.

[3] Hargreaves B a., Cunningham CH, Nishimura DG, Conolly SM. Variable-rate selective excitation for rapid MRI sequences. Magn Reson Med. 2004;52(3):590–7.

[4] Middione MJ, Wu HH, Ennis DB. Convex gradient optimization for increased spatiotemporal resolution and improved accuracy in phase contrast MRI. Magn Reson Med. 2014;72(6):1552–64.

[5] Franz X. Hebrank, Matthias Gebhardt. SAFE-Model - A New Method for Predicting Peripheral Nerve Stimulations in MRI. ISMRM. 2000.

Figures

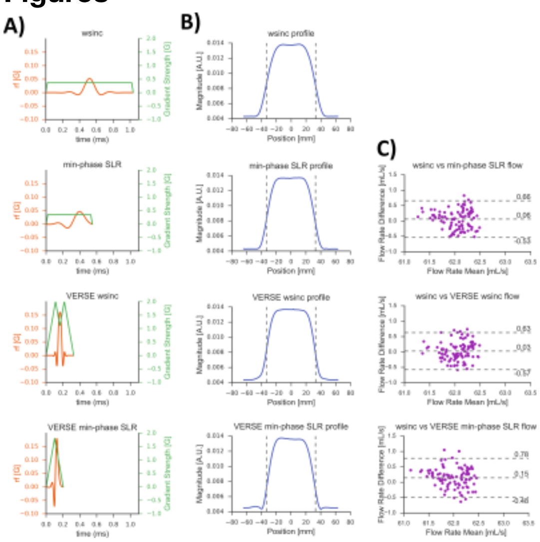

The left column (A) shows the RF and gradient waveforms of the tested slab-excitation pulses. The middle column (B) shows the slab excitation profile as measured in a phantom. The right column (C) shows the Bland-Altman comparison of flow values relative to the reference excitation. The rows from top to bottom are: The reference windowed sinc excitation, a minimum-phase SLR excitation, a VERSE optimized windowed sinc (matching the reference), and a VERSE optimized minimum-phase SLR.

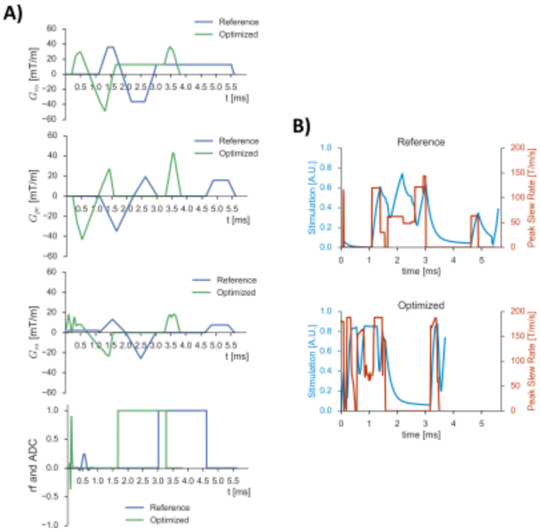

(A) Gradient waveforms, RF, and ADC events for the reference and optimized waveforms for the protocol used in the flow phantom and in vivo experiments. The optimized sequence has a shorter excitation waveform, shorter bipolars, and shorter spoilers. (B) Relationship between PNS and peak slew rate for the reference and optimized sequences. The optimized sequence more frequently uses the maximum slew-rate while balancing slewing with the PNS limit.

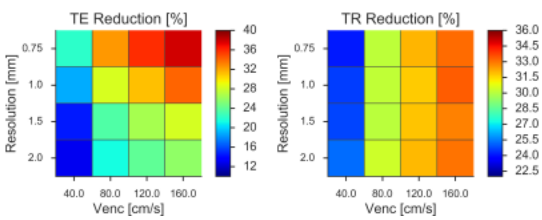

TE and TR reductions for protocols spanning a range of Vencs and isotropic resolutions. TE and TR were reduced by 13-38% and 24-33% respectively.

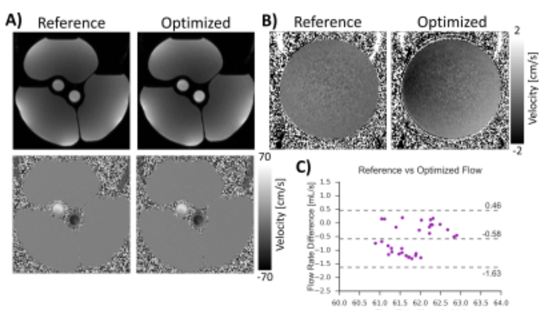

(A) Magnitude and through plane velocity images form the flow phantom for both sequences; no noticeable differences were seen. (B) Velocity images from a static phantom that was placed off-isocenter. Images are shown with a very narrow dynamic range to highlight the slightly increased eddy currents seen with the optimized method. (C) Bland-Altman comparison of the flow values measured from vessels seen in (A).

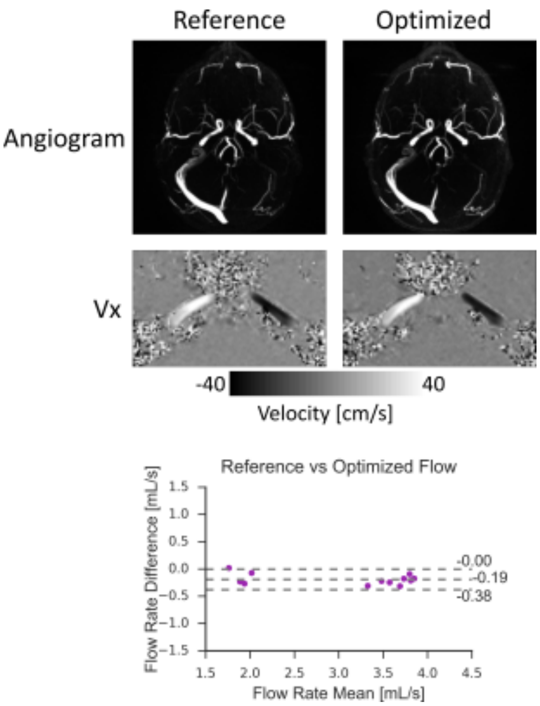

The results of the volunteer experiment. The first row shows the calculated angiograms from the data, where little difference is seen in the images. The second row shows a cropped axial slice from the x-velocity dataset in the carotid siphon, where no qualitative difference is seen. The Bland-Altman comparison shows flow rates measured at multiple slices in the ICA and basilar artery and shows a bias of -0.19 mL/s and LOA of -0.38 to 0.00 mL/s.